Quadratic Programming-based Electric Vehicle Charging Optimisation combining Charging Cost and Grid Power Peak Minimisation

Branimir Škugor[1], Jakov Topić and Joško Deur
University of Zagreb, Faculty of Mechanical Engineering and Naval Architecture
Ivana Lučića 5, 10002 Zagreb, Croatia
[1]Corresponding author, Email: branimir.skugor@fsb.hr

Abstract

This paper deals with charging optimisation of an electric vehicle (EV) fleet, which is aimed at real-time applications which includes both charging cost and peak power minimisation. It is shown that the optimal charging problem which includes these two criteria can be modelled as a quadratic optimisation problem, and can, thus, be solved with widely available and computationally efficient quadratic programming solvers. The corresponding quadratic cost function is extended with a single, free parameter, in order to enable tuning of relative significance of charging cost- and peak power-related sub-cost functions. The functionality of the proposed charging optimisation approach is demonstrated for the case of an isolated electrical energy system and hypothetical EV fleet of the National park Mljet. The time distributions, needed as inputs for charging optimisation, are obtained by using appropriate EV models and available driving cycles and related schedules of the particular fleet. Finally, benefits of using the presented charging optimisation method are presented based on comparison with respect to uncontrolled charging (charge when connected) results in terms of charging cost and peak power values.

Keywords

Load levelling, charging cost minimisation, linear/quadratic programing, modelling, electric vehicle fleet, isolated energy system.

1. Introduction

The isolated electric grid systems, such as those present on islands, are usually characterised by a limit grid power and highly fluctuating load. Introduction of electric vehicles (EV) can make the situation even worse if the EV charging is managed poorly (e.g. charge when connected) [1]. Therefore, an advanced EV charging management is of a great significance for those applications. In general, the aim is to optimise charging schedule of a fleet of EVs in order to level the overall grid load to a large extent, and at the same time to reduce the energy cost.

The EV fleet charging optimisation is mainly studied from the perspective of charging cost minimisation, while the grid load levelling and other EV fleet-related benefits can be indirectly achieved to some extent [2, 3]. For instance, in the case where the charging cost is the only objective, the grid load levelling and other target benefits can be achieved by appropriately varying the electrical energy price. These optimisation problems are mostly modelled as linear problems, what derives from simple (linear) battery models and the assumption that the EV charging does not affect the electrical energy price [4, 5]. However, in the scenario of the EV fleet charging affecting the electrical energy price and the linear relation between these two variables exists, the linear optimisation problem transfers to the quadratic one [6], while in the case of even more complex relations, the problem transfers to the nonlinear one which can be solved by SQP optimisation technique [7] or a game theory-based approach [8]. Similarly, in the case of more complex battery model, the optimisation problem also transfers towards the quadratic or nonlinear ones [5]. Furthermore, the EV charging optimisation can be solved within model predictive control (MPC) framework, as it is demonstrated in [9], where the battery is represented by a linear model, and the optimisation is modelled as a mixed integer linear program (MILP) in order to account for the real charger power limitations (i.e. semi-continuous charging). Apart from the optimisation on the individual EV level, in [10] and [11] the charging optimisations are conducted on the EV fleet level by using dynamic programming (DP) algorithm, where an EV fleet is modelled as an aggregate battery with the aim of minimising the charging cost only. On the other hand, the load levelling is directly performed by using a genetic algorithm-based optimisation in [12], where the load levelling is achieved by minimising the difference between adjacent charging power values. However, in [12] the objective function does not include the charging cost which is important from the standpoint of the user.

In this paper, the combined EV fleet charging problem including both the charging cost and the grid power peak minimisation is proposed. First, the problem is formulated as a linear optimisation problem, where both cost function and constraints are linear, and only the cost of electrical energy used for charging is minimized. To this end, the state equations and constraints related to EVs (e.g. the battery state of charge and charging power limits) are adapted and expressed in the linear programming matrix form. Next, the basic linear optimisation problem is extended to the quadratic optimisation problem in order to minimise the grid power peak along with the charging cost. The grid power peak minimisation represents the standard min-max optimisation problem which is proven for this particular case to be equivalent to the derived quadratic optimisation problem with a quadratic cost function and linear constraints. Finally, a free parameter determining the relative significance between the two sub-cost functions (related to the charging cost and the peak power) is introduced within the quadratic cost function in order to enable the charging optimisation problem to be customized for the target system.

The proposed EV charging optimisation methods are applied for the case of the National park Mljet, where conventional vehicle fleet is virtually replaced with electric one (including electric cars, trucks, mini-buses, tourist trains, and boats). The time distributions required for parameterisation of the charging optimisation algorithms are obtained by using appropriate EV models and available driving cycles and related schedules of the particular fleet, and assumptions related to the corresponding specific energy consumptions. Finally, the linear and quadratic charging optimisations are conducted and compared with each other in terms of (i) charging cost and (ii) load levelling.

The main contributions of the paper are: (i) formulating the optimal charging problem in the way to explicitly involve both the charging cost and the grid power peaks aimed to be minimised, (ii) the proof that the combined grid power peak and the energy cost minimisation can be represented as a quadratic optimisation problem, and (iii) proposing an extension of the quadratic cost function with a free parameter and normalising constants in order to enable customised tuning of the charging algorithm.

2. Electric vehicle fleet

This section first gives the basic description of the EV fleet predicted to replace the conventional vehicle fleet currently used in the National park Mljet. Then, the individual battery model needed for the charging optimisation algorithm described in Section 3 is given and parameterised for the case of the considered EV fleet.

2.1. EV fleet and electrical energy system description

The vehicles within considered conventional vehicle fleet can be divided into several categories according to their usage characteristics: (i) light vehicles, (ii) medium duty vehicles, and (iii) mini-buses. Apart from replacing the existing vehicles, the introduction of electric trains and electric boats is also planned in the near future. The chosen electric counterparts of the existing conventional vehicles are listed in Table 1, along with the corresponding basic parameters (max. charging power and battery capacity) important from the standpoint of the charging control algorithm. Also, the estimated specific energy consumptions λ (kWh per travelled distance given in km) are given along with the estimated total daily distance travelled L_{daily}.

The electrical infrastructure on the island is planned to be upgraded in the scenario of EV introduction in order to be able to cover significantly higher loads caused by EVs and it's power capacity is predicted to be in the range from 70 to 100 kW. Here, the grid power limit ($P_{grid,limit}$) of 75 kW is assumed.

It can be seen that the possible aggregate charging power peak of 11 EVs in the scenario of slow charging (the last row of Table 1) is very close to the assumed grid power limit, ≈73 kW vs. 75 kW. This limit could be easily violated in the presence of other electrical consumers, or in the scenario of fast charging, if an uncontrolled charging of EV fleet is applied. On the other hand, the aggregate battery capacity of 670 kWh represents the significant storage from the perspective of grid, which can be used and fully exploited for the grid load levelling if the EV fleet charging is controlled in an optimal way.

Table 1. List of hypothetical EVs predicted to replace current conventional vehicles in the National park Mljet along with the corresponding basic parameters.

Vehicle	Quantity	P_{cmax} [kW]***	E_{max} [kWh]	λ [kWh/km]	L_{daily} [km]
Mitsubishi iMIEV	1	3.0	16.0	0.21	125
Mitsubishi Outlander PHEV	1	3.0	12.0	0.23	52
VW Golf GTE	1	3.6	8.7	0.18	50
Mini-bus A	2	10.0 (22.0*)	84.0	-	-
Mini-bus B	2	10.0 (22.0*)	84.0	-	-
Nissan e-NV200	1	3.3 (6.6*)	24.0	0.20	50
Electric train 1	2	5.0 (10.0*)	56.0	0.79	79.6
Electric train 2	2	5.0 (10.0*)	56.0	0.78	44.74
Electric boat (1,2,3)	3	10.0	110.0	N.A.	N.A.
Aggregate	11	72.9 (110.2) **	670.7**	-	-

**Maximum charging power in the case of fast charging*
***Maximum aggregate charging power and aggregate battery capacity are calculated by multiplying a number of EVs with corresponding individual battery capacity and summing over all types of vehicles (e.g. 2 mini-buses contribute to aggregate battery capacity with 168 kWh (2x84 kWh))*
****P_{cmax} – max. charging power, E_{max} – battery capacity, λ - specific energy consumption, L_{daily} - estimated daily distance travelled*

The other consumers considered in this case study include: (i) one lift of average power of 11.04 kW, (ii) public lights of average power of 4.6 kW, and (iii) the aggregated electrical consumers of one building of average power of 11.04 kW. In order to obtain the aggregate power time profile, it is assumed that the lift does not operate over night, while the public lights are turned off during the day and vice versa. This brings the total aggregate power of 15.7 kW during the period from 0-6h, and 21-24h; and power of 22.1 kW during the rest of the day (6-21h).

2.2. Individual battery model

The batteries of individual EVs listed in Table 1 are modelled as an energy storage with a state of charge (SoC) as a single state variable. The battery dynamics is described by the discrete-time state equation [13]

$$SoC_i(k+1) = SoC_i(k) + \eta_{ch,i}\frac{\left(P_{c,i}(k) + P_{reg,i}(k)\right)\Delta T}{E_{\max,i}} - \frac{P_{dem,i}(k)\Delta T}{\eta_{dch,i}E_{\max,i}}\ , \tag{1}$$

where $P_{c,i}$ represents the battery charging power (charging from the grid), $P_{reg,i}$ regenerative braking power (charging from the road), and $P_{dem,i}$ demanded power needed for vehicle propulsion (discharging) for i^{th} EV within k^{th} discrete time step. The energy capacity of battery is denoted with $E_{\max,i}$, while the corresponding charging and discharging efficiencies are denoted with η_{ch} and η_{dch}, respectively. ΔT represents time discretisation.

The state variable SoC is assumed to take values in range between 0 and 1, with the lower limit ($SoC_{\min}$) typically posed above 0, and the upper limit $SoC_{\max}$ below 1 with the motivation to extend a battery lifetime.

$$0 \le SoC_{\min} \le SoC_i(k) \le SoC_{\max} \le 1. \tag{2}$$

Here, the battery charging power is limited to positive values (i.e. power flow only from the grid to EV) with the upper limit of i^{th} EV depending on the maximum charging power $P_{c\max,i}$ and the time share of EV being connected to the grid within k^{th} discrete time step $n_{dc,i}(k)$ ($0 \le n_{dc,i} \le 1$; e.g. $n_{dc,i} = 0.5$ means that i^{th} EV is connected to the grid for the half of time within k^{th} time step).

$$0 \le P_{c,i}(k) \le n_{dc,i}(k) P_{c\max,i}\,. \tag{3}$$

The aggregate charging power is calculated by summing up individual charging powers of all EVs within fleet for each discrete time step k as follows

$$P_{c,agg}(k) = \sum_{i=1}^{N_v} P_{c,i}(k), \quad k = 0,1,\,2,\,...,N_t - 1, \tag{4}$$

where N_v denotes the total number of EVs within fleet, and N_t the total number of discrete time steps.

2.3. Parameterisation of battery models

According to the given battery model, the following discrete time distributions of i^{th} EV should be calculated: (i) the regenerative braking power ($P_{reg,i}$), (ii) the demanded driving power ($P_{dem,i}$), (iii) the time share of EV being connected to the grid within discrete time step ($n_{dc,i}$), and (iv) the time steps when EV is being disconnected from the grid $n_{dc,o,i}$ ($n_{dc,o,i}(k)$ = 1 if i^{th} EV is disconnected within the time step k, otherwise it is zero). The discretisation time is set to 1 hour (ΔT = 1h), and the total time horizon on which the charging optimisation is conducted to 24h (N_t = 24).

Table 2 shows the 24-hour time distribution of the demanded power P_{dem} for each EV within fleet. These distributions are in the case of mini-buses and electric trains obtained from the simulations of the corresponding simple quasi-static models over assumed driving cycles, while in the case of other EVs they are calculated based on the predicted EV tasks, i.e. time schedules of target routes with known travelled distance, and assumed specific energy consumption (see λ in Table 1). For the sake of simplicity, it is assumed that the regenerative braking functionality is not available and the time distribution $P_{reg,i}(k)$ is set to 0 for each time step k and each EV. Table 2 also contains the time distribution n_{dc} for each EV in the form of a cell colour. The blue cells correspond to the periods when an EV is connected to the grid (n_{dc} = 1 for all blue cells with the exceptions of $n_{dc}(9)=n_{dc}(21)=0.5$ for the case of Mitsubishi iMIEV), while the red ones correspond to the driving periods (n_{dc}=0). The distributions of time steps when an EV is being disconnected from the grid $n_{dc,o}$ are given later (dark blue cells in Table 3).

Table 2. Time distributions of connection to the grid (blue cell = EV connected to the grid, red cell = EV driving and not connected to the grid) and power demands for each EV.

Distribution P_{dem} [kW]	**0**	**1**	**2**	**3**	**4**	**5**	**6**	**7**	**8**	**9**	**10**	**11**	**12**	**13**	**14**	**15**	**16**	**17**	**18**	**19**	**20**	**21**	**22**	**23**
Mitsubishi iMIEV	4.8	0	0	0	0	0	4.8	0	0	2.5	0	0	4.8	0	0	0	0	0	4.8	0	0	4.4	0	0
Mitsubishi Outlander	0.6	0.6	0.6	0.3	0.3	0.6	0.6	0.6	0	0	0	0	0	0.6	0.6	0.6	0.6	0.6	0.6	0.6	0.6	0.6	0.3	0.3
VW Golf GTE	0.4	0.4	0.4	0.4	0.4	0.4	0.4	0	0	0	0	0.4	0.4	0.4	0.4	0.4	0.4	0.4	0.4	0.4	0.4	0.4	0.2	0.2
Mini-bus A	0	0	0	0	0	0	0	0	5.3	7.7	12.7	13.2	10.1	4.0	0	5.9	12.2	9.6	0	0	0	0	0	0
Mini-bus B	0	0	0	0	0	0	0	0	0	0	12.5	12.9	0	3.2	6.4	8.0	12.5	12.1	9.1	5.7	7.9	0	0	0
Nissan e-NV200	0	0	0	0	0	0	0	0	2	0	0	0	0	2	1	0	0	0	2	2	1	0	0	0
Electric train 1	0	0	0	0	0	0	0	0	0	6.3	6.3	6.3	6.3	6.3	6.3	0	0	6.3	6.3	6.3	6.3	0	0	0
Electric train 2	0	0	0	0	0	0	0	0	2.7	2.7	2.7	2.7	2.7	2.7	2.7	2.7	2.7	2.7	2.7	2.7	2.7	0	0	0
Electric boat	0	0	0	0	0	0	0	6.5	6.5	6.5	6.5	6.5	6.5	6.5	6.5	6.5	6.5	6.5	6.5	6.5	6.5	0	0	0
Electric boat	0	0	0	0	0	0	0	6.5	6.5	6.5	6.5	6.5	6.5	6.5	6.5	6.5	6.5	6.5	6.5	6.5	6.5	0	0	0
Electric boat	0	0	0	0	0	0	0	6.5	6.5	6.5	6.5	6.5	6.5	6.5	6.5	6.5	6.5	6.5	6.5	6.5	6.5	0	0	0

By aggregating the distributions given in Table 2, the 24h-time distributions of number of EVs connected to the grid ($n_{dc,agg}$) and the aggregate driving power demand ($P_{dem,agg}$) are obtained and shown in Fig. 1. In Fig. 1a, it can be seen that during morning and evening hours (0:00h-6:00h and 21:00h-24:00h) most of the EVs are predicted to be connected to the grid and thus available for charging, while during the day most of them will be driving and thus causing the relatively high power demand (Fig. 1b).

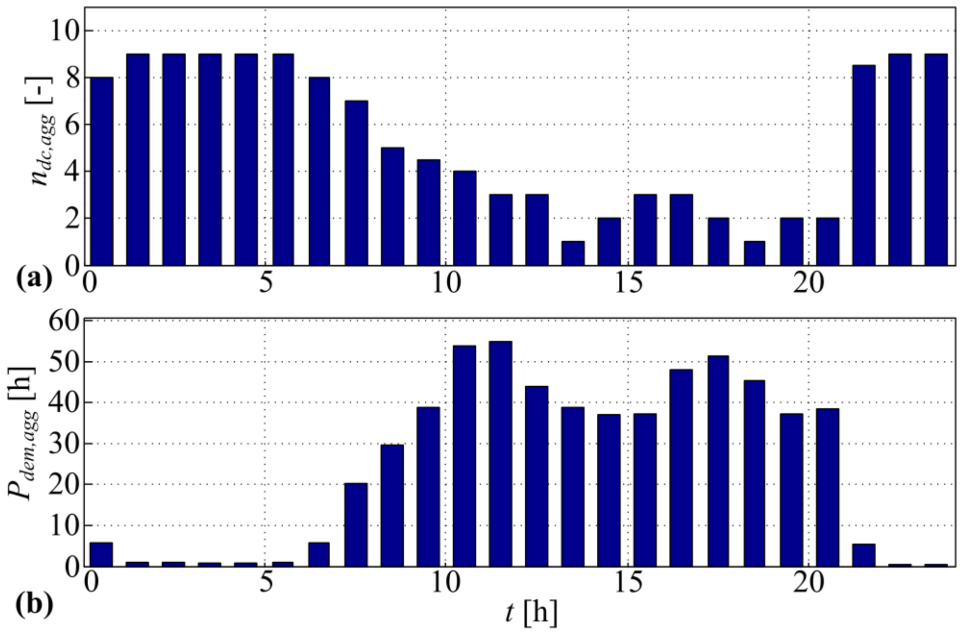

Figure 1. Time distributions of total number of EVs connected to the grid $n_{dc,agg}$ (a), and aggregated EV power demand $P_{dem,agg}$ (b).

3. Minimisation of EV fleet charging cost

3.1. Optimal control problem formulation

The cost function J denoting the cost of electrical energy taken from the grid and aimed to be minimised is calculated as follows

$$J = \sum_{k=0}^{N_t-1} C_{el}(k) \frac{P_{grid}(k)\Delta T}{1000}, \quad k = 0, 1, 2, ..., N_t - 1, \tag{5}$$

where $C_{el}(k)$ term represents the unit cost of electrical energy (HRK/kWH; HRK denotes Croatian monetary unit), while the term $P_{grid}(k)\Delta T/1000$ represents energy taken from the grid and expressed in kWh for the k^{th} discrete time step. The optimisation is subject to EVs SoC- (2) and charging power-related constraints (3). The grid power is calculated as

$$P_{grid}(k) = P_{c,agg}(k) + P_{O.C.}(k), \quad k = 0, 1, 2, ..., N_t - 1 \tag{6}$$

where $P_{c,agg}$ represents the aggregate charging power of EV fleet (4) and $P_{O.C.}$ the aggregate power of other electrical consumers within the considered electrical energy system.

3.2. Optimal control problem represented in linear programming (LP) form

The optimal control problem given by equations (5), (2) and (3) is linear both in a cost function and constraints and can be represented by the general LP form given by [14]

$$\min \ \mathbf{c}^T\mathbf{x}, \quad \text{s.t.}\ A\mathbf{x} \le \mathbf{b}, \tag{7}$$

where $\mathbf{c}$ is a weighting vector typically containing unit costs, $\mathbf{x}$ is a vector to be determined in order to minimise a cost function $\mathbf{c}^T\mathbf{x}$, and $A\mathbf{x} \le \mathbf{b}$ are linear constraints given in matrix form.

In order to transform individual EV-related constraints given by (2) and (3) to matrix form $A\mathbf{x} \leq \mathbf{b}$ from (7), the following variables are introduced:

$$\mathbf{x}_i = \left[P_{c,i}(0) \quad P_{c,i}(1) \quad \ldots \quad P_{c,i}(N_t - 1)\right]^T, \tag{8a}$$

$$\mathbf{x} = \left[\mathbf{x}_1{}^T \, \mathbf{x}_2{}^T \ldots \mathbf{x}_{N_v}{}^T\right]^T, \tag{8b}$$

$$\mathbf{b}_i = \left[n_{dc,i}(0) \quad n_{dc,i}(1) \quad \ldots \quad n_{dc,i}(N_t - 1)\right]^T, \tag{9a}$$

$$\mathbf{b} = \left[\mathbf{b}_1{}^T \, \mathbf{b}_2{}^T \ldots \mathbf{b}_{N_v}{}^T\right]^T; \tag{9b}$$

where $\mathbf{x}_i$ denotes the vector of length N_t containing the charging power of i^{th} EV for each discrete time step, and the vector $\mathbf{x}$ contains the charging power vectors $\mathbf{x}_i$ of all individual EVs. In the same way, the vector $\mathbf{b}_i$ contains the time share of i^{th} EV being connected to the grid within each time step, while the vector $\mathbf{b}$ contains all individual EV time shares $\mathbf{b}_i$, i.e. of all EVs within fleet.

3.2.1. Matrix form of individual EV-related constraints

By combining equations (8a) and (9a), equation (3) can be represented as

$$\underbrace{\frac{1}{P_{c\max,i}} I}_{A_i} \mathbf{x}_i \leq \mathbf{b}_i, \tag{10}$$

thus corresponding to the form of LP constraint $A_i\mathbf{x}_i \leq \mathbf{b}_i$.

Recursive state equation (1) can be rewritten as follows

$$SoC_i(k) = SoC_i(0) + \frac{\eta_{ch} \cdot \Delta T}{E_{\max}} \sum_{j=0}^{k-1} P_{c,i}(j) + \frac{\eta_{ch} \cdot \Delta T}{E_{\max}} \sum_{j=0}^{k-1} P_{reg,i}(j) - \frac{\Delta T}{\eta_{dch} E_{\max}} \sum_{j=0}^{k-1} P_{dem,i}(j) \tag{11}$$

By posing

$$\mathbf{y}_i = \left[SoC_i(1) \quad SoC_i(2) \quad \ldots \quad SoC_i(N_t)\right], \tag{12}$$

the state equation (1) can be written in the form

$$\mathbf{y}_i = B_i \mathbf{x}_i + \mathbf{d}_i, \tag{13}$$

where matrix B_i is calculated as (D_{LT} is lower triangular matrix of dimensions $N_t \mathrm{x} N_t$):

$$B_i = \frac{\eta_{ch} \cdot \Delta T}{E_{\max}} D_{LT}, \tag{14}$$

and elements (denoted by index k) of vector $\mathbf{d}_i$ as:

$$d_{i,k} = SoC_i(0) + \frac{\eta_{ch} \cdot \Delta T}{E_{\max}} \sum_{j=0}^{k-1} P_{reg,i}(j) - \frac{\Delta T}{\eta_{dch} E_{\max}} \sum_{j=0}^{k-1} P_{dem,i}(j) \tag{15}$$

Then, equation (2) can be written as

$$SoC_{\min} \le B_i \mathbf{x}_i + \mathbf{d}_i \le SoC_{\max} \tag{16}$$

and further as

$$-B_i \mathbf{x}_i \le \mathbf{d}_i - SoC_{\min}\,, \tag{17}$$

$$B_i \mathbf{x}_i \le SoC_{\max} - \mathbf{d}_i\,. \tag{18}$$

The constraints (17) and (18) are now joined to the constraint (10) in the general LP form of constraints as follows:

$$\underbrace{\begin{bmatrix} A_i \\ -B_i \\ B_i \end{bmatrix}}_{A_{ineq,i}} \mathbf{x}_i \le \underbrace{\begin{bmatrix} \mathbf{b}_i \\ \mathbf{d}_i - SoC_{\min} \\ SoC_{\max} - \mathbf{d}_i \end{bmatrix}}_{b_{ineq,i}}, \tag{19}$$

Furthermore, in order to achieve target (predefined) SoC value of each EV at the end of each charging period, the additional equality constraint is introduced along with the existing constraints (19). First, the state equation (11) is modified as

$$SoC_{\mathrm{mod},i}(k) = SoC_i(0) + \frac{\eta_{ch} \cdot \Delta T}{E_{\max}} \sum_{j=0}^{k-1} P_{c,i}(j) + \frac{\eta_{ch} \cdot \Delta T}{E_{\max}} \sum_{j=0}^{k-2} P_{reg,i}(j) - \frac{\Delta T}{\eta_{dch} E_{\max}} \sum_{j=0}^{k-2} P_{dem,i}(j)\,, \tag{20}$$

in order to take into account causality condition of EV charging. In this way, modified SoC (SoC_{mod}) in k^{th} discrete time step does not include values $P_{reg,i}$ and $P_{dem,i}$ from the $(k-1)^{th}$ discrete time step as opposed to the equation (11). This modified SoC value is required to be equal to the target value in the time steps when corresponding EV disconnects from the grid ($SoC_{mod}(k) = SoC_{target}$ for the case $n_{dc,o,i}(k-1) = 1$). By excluding $P_{reg,i}(k-1)$ and $P_{dem,i}(k-1)$ from the calculation of SoC in equation (20), non-causal covering of driving power $P_{dem,i}(k-1)$, which happens after EV has been disconnected from the grid and started driving, with charging power from the grid $P_{c,i}$ within the same $(k-1)^{\mathrm{th}}$ time step, is avoided. Then, modified version of equations (12)-(15) are introduced

$$\mathbf{y}_{\mathrm{mod},i} = \left[SoC_{\mathrm{mod},i}(1) \quad SoC_{\mathrm{mod},i}(2) \quad \ldots \quad SoC_{\mathrm{mod},i}(N_t) \right], \tag{21}$$

$$\mathbf{y}_{\mathrm{mod},i} = B_i \mathbf{x}_i + \mathbf{d}_{\mathrm{mod},i}\,. \tag{22}$$

Based on the equation (20), $d_{mod,i}$ from equation (22) is calculated as

$$d_{\mathrm{mod},i,k} = SoC_i(0) + \frac{\eta_{ch} \cdot \Delta T}{E_{\max}} \sum_{j=0}^{k-2} P_{reg,i}(j) - \frac{\Delta T}{\eta_{dch} E_{\max}} \sum_{j=0}^{k-2} P_{dem,i}(j)\,. \tag{23}$$

Due to causality condition and physical constraint ($SoC \le 1$), in the step k when EV is disconnecting from the grid ($n_{dc,o,i,k} = 1$), the following constraint should be satisfied

$$(B_i \mathbf{x}_i)_k + d_{\mathrm{mod},i,k} \le 1, \text{ for } n_{dc,o,i,k} = 1\,. \tag{24}$$

This inequality constraint can be represented as an equality constraint by demanding the particular target SoC value of each EV when disconnecting:

$$diag(\mathbf{n}_{dc,o,i}) \cdot (B_i \mathbf{x}_i + \mathbf{d}_{\mathrm{mod},i}) = SoC_{target} \mathbf{n}_{dc,o,i}, \tag{25}$$

where $diag(\mathbf{n}_{dc,o,i})$ represents diagonal matrix containing the values of vector $\mathbf{n}_{dc,o,i}$ as the main diagonal elements. By arranging this equation, the standard form of linear equality constraint is obtained as follows:

$$\underbrace{diag(\mathbf{n}_{dc,o,i}) \cdot B_i}_{A_{eq,i}} \mathbf{x}_i = \underbrace{SoC_{target} \mathbf{n}_{dc,o,i} - diag(\mathbf{n}_{dc,o,i}) \cdot \mathbf{d}_{\mathrm{mod},i}}_{b_{eq,i}} \tag{26}$$

Additionally, in order to satisfy requirement on the SoC value at the end of optimisation time horizon to be equal to SoC_{target} value (for the last discrete time step $k = N_t$), the last element of the vector $\mathbf{n}_{dc,o,i}$ is set to 1 ($\mathbf{n}_{dc,o,i}(N_t-1) = 1$) although EV is not being disconnected from the grid in that time step.

3.2.2. Matrix form of EV fleet constraints

Inequality and equality constraints for the whole EV fleet ($i = 1, 2, ..., N_v$) are derived from the individual EV-related ones (19) and (26) as follows:

$$\underbrace{\begin{bmatrix} A_{ineq,1} & 0 & \cdots & 0 \\ 0 & A_{ineq,2} & \cdots & 0 \\ \vdots & \vdots & \ddots & \vdots \\ 0 & 0 & \cdots & A_{ineq,N_v} \end{bmatrix}}_{A_{ineq}} \underbrace{\begin{bmatrix} \mathbf{x}_1 \\ \mathbf{x}_2 \\ \vdots \\ \mathbf{x}_{N_v} \end{bmatrix}}_{\mathbf{x}} \leq \underbrace{\begin{bmatrix} \mathbf{b}_{ineq,1} \\ \mathbf{b}_{ineq,2} \\ \vdots \\ \mathbf{b}_{ineq,N_v} \end{bmatrix}}_{\mathbf{b}_{ineq}}, \tag{27}$$

$$\underbrace{\begin{bmatrix} A_{eq,1} & 0 & \cdots & 0 \\ 0 & A_{eq,2} & \cdots & 0 \\ \vdots & \vdots & \ddots & \vdots \\ 0 & 0 & \cdots & A_{eq,N_v} \end{bmatrix}}_{A_{eq}} \underbrace{\begin{bmatrix} \mathbf{x}_1 \\ \mathbf{x}_2 \\ \vdots \\ \mathbf{x}_{N_v} \end{bmatrix}}_{\mathbf{x}} = \underbrace{\begin{bmatrix} \mathbf{b}_{eq,1} \\ \mathbf{b}_{eq,2} \\ \vdots \\ \mathbf{b}_{eq,N_v} \end{bmatrix}}_{\mathbf{b}_{eq}}. \tag{28}$$

Dimensions of control vector $\mathbf{x}$ are ($N_t \cdot N_v$, 1), of matrices A_{eq} and A_{ineq} ($N_t \cdot N_v$, $N_t \cdot N_v$), and of vectors $\mathbf{b}_{eq}$ and $\mathbf{b}_{ineq}$ ($N_t \cdot N_v$, 1).

3.2.3. Linear cost function

According to equation (5), the total cost of electrical energy taken from the grid is aimed to be minimised. The unit cost of electrical energy C_{el} is rewritten to the vector form as

$$\mathbf{c}_i = \frac{1}{1000} \left[C_{el}(0) \quad C_{el}(1) \quad ... \quad C_{el}(N_t - 1) \right]^T, \forall i \tag{29}$$

$$\mathbf{c} = \left[\mathbf{c}_1{}^T \, \mathbf{c}_2{}^T \, ... \, \mathbf{c}_{N_v}{}^T \right]^T, \tag{30}$$

where scaling factor of 1/1000 is used in order to transform the unit cost given in HRK/kWh to HRK/Wh since the control vector **x** contains the electrical power expressed in the unit W. Based on this, the LP-like cost function $\mathbf{c}^{\mathrm{T}}\mathbf{x}\Delta T$ follows (see (7)), where $\mathbf{x}\Delta T$ represents the charging energy vector (the multiplication of power **x** and discretisation time ΔT yields energy).

In order to include the power consumption of other electrical consumers $P_{O.C.}$ (see (6)) in the optimisation problem, the following vector whose elements represent the corresponding aggregate power for each discrete time step is introduced:

$$\mathbf{x}_{O.C.} = \begin{bmatrix} P_{O.C.}(0) & P_{O.C.}(1) & \dots & P_{O.C.}(N_t - 1) \end{bmatrix}^T . \tag{31}$$

Then, the control vector (8b) containing the charging power of each EV is extended to include the aggregate power of other electrical consumers.

$$\mathbf{x} = \begin{bmatrix} \mathbf{x}_1^{\ T} \ \mathbf{x}_2^{\ T} \dots \mathbf{x}_{N_v}^{\ T} \ \mathbf{x}_{O.C.}^{\ T} \end{bmatrix}^T . \tag{32}$$

Due to this, the cost vector **c** from (30) is also extended as

$$\mathbf{c}_{O.C.} = \frac{1}{1000}\begin{bmatrix} C_{el}(0) & C_{el}(1) & \dots & C_{el}(N_t - 1) \end{bmatrix}^T , \tag{33}$$

$$\mathbf{c} = \begin{bmatrix} \mathbf{c}_1^{\ T} \ \mathbf{c}_2^{\ T} \dots \mathbf{c}_{N_v}^{\ T} \ \mathbf{c}_{O.C.}^{\ T} \end{bmatrix}^T . \tag{34}$$

The equality constraint (28) is modified in order to account for the extended control vector **x** as follows

$$\underbrace{\begin{bmatrix} A_{eq,1} & 0 & \dots & 0 & 0 \\ 0 & A_{eq,2} & \dots & 0 & 0 \\ \vdots & \vdots & \ddots & \vdots & \vdots \\ 0 & 0 & \dots & A_{eq,N_v} & 0 \\ 0 & 0 & \dots & 0 & A_{eq,O.C.} \end{bmatrix}}_{A_{eq}} \underbrace{\begin{bmatrix} \mathbf{x}_1 \\ \mathbf{x}_2 \\ \vdots \\ \mathbf{x}_{N_v} \\ \mathbf{x}_{O.C.} \end{bmatrix}}_{\mathbf{x}} = \underbrace{\begin{bmatrix} \mathbf{b}_{eq,1} \\ \mathbf{b}_{eq,2} \\ \vdots \\ \mathbf{b}_{eq,N_v} \\ \mathbf{x}_{O.C.} \end{bmatrix}}_{\mathbf{b}_{eq}} . \tag{35}$$

The matrix $A_{eq,O.C.}$ is a unit matrix (only non-zero elements of unit values are contained on the main matrix diagonal). This is set in this way because the power consumption of other electrical consumers is considered to be non-flexible, i.e. uncontrollable.

Due to the extension of the control vector **x**, the inequality matrix A_{ineq} from (27) is extended with zero elements as follows:

$$\underbrace{\begin{bmatrix} A_{ineq,1} & 0 & \dots & 0 & 0 \\ 0 & A_{ineq,2} & \dots & 0 & 0 \\ \vdots & \vdots & \ddots & \vdots & \vdots \\ 0 & 0 & \dots & A_{ineq,N_v} & 0 \end{bmatrix}}_{A_{ineq}} \underbrace{\begin{bmatrix} \mathbf{x}_1 \\ \mathbf{x}_2 \\ \vdots \\ \mathbf{x}_{N_v} \\ \mathbf{x}_{O.C.} \end{bmatrix}}_{\mathbf{x}} \leq \underbrace{\begin{bmatrix} \mathbf{b}_{ineq,1} \\ \mathbf{b}_{ineq,2} \\ \vdots \\ \mathbf{b}_{ineq,N_v} \end{bmatrix}}_{\mathbf{b}_{ineq}} . \tag{36}$$

In order to include the constraint related to the maximum aggregate power which can be drawn from the grid $P_{grid,\max}$, the following relation is introduced

$$\left[P_{grid}(0) \quad P_{grid}(1) \quad \dots \quad P_{grid}(N_t - 1)\right]^T = H\mathbf{x}, \tag{37}$$

where the time distribution of aggregate grid power $P_{grid}(k)$ is calculated from the control vector $\mathbf{x}$ via matrix H. The matrix H is formed as

$$H = \begin{bmatrix} \mathbf{p}_{1,1} & \mathbf{p}_{1,2} & \cdots & \mathbf{p}_{1,N_v} & \mathbf{p}_{1,N_v+1} \\ \mathbf{p}_{2,1} & \mathbf{p}_{2,2} & \cdots & \mathbf{p}_{2,N_v} & \mathbf{p}_{2,N_v+1} \\ \vdots & \vdots & \ddots & \vdots & \vdots \\ \mathbf{p}_{N_t,1} & \mathbf{p}_{N_t,2} & \cdots & \mathbf{p}_{N_t,N_v} & \mathbf{p}_{N_t,N_v+1} \end{bmatrix}, \tag{38}$$

whose element in the j^{th} row and the i^{th} column $\mathbf{p}_{j,i}$ represents the row-vector of N_t elements, where only j^{th} element is non-zero, i.e. set to 1.

Then, the maximum grid power constraint $P_{grid}(k) \leq P_{grid,\max}$ is joined to other inequality constraints (43) as follows

$$\underbrace{\begin{bmatrix} A_{ineq,1} & 0 & \dots & 0 & 0 \\ 0 & A_{ineq,2} & \dots & 0 & 0 \\ \vdots & \vdots & \ddots & \vdots & \vdots \\ 0 & 0 & \dots & A_{ineq,N_v} & 0 \\ & & H & & \end{bmatrix}}_{A_{ineq}} \underbrace{\begin{bmatrix} \mathbf{x}_1 \\ \mathbf{x}_2 \\ \vdots \\ \mathbf{x}_{N_v} \\ \mathbf{x}_{O.C.} \end{bmatrix}}_{\mathbf{x}} \leq \underbrace{\begin{bmatrix} \mathbf{b}_{ineq,1} \\ \mathbf{b}_{ineq,2} \\ \vdots \\ \mathbf{b}_{ineq,N_v} \\ \mathbf{P}_{grid,\max} \end{bmatrix}}_{\mathbf{b}_{ineq}}. \tag{39}$$

The vector $\mathbf{P}_{grid,\max}$ contains the constants $P_{grid,\max}$ and it's number of elements corresponds to the number of discrete time steps N_t.

The final linear charging optimisation problem

$$\min\ \mathbf{c}^T\mathbf{x}\Delta T, \quad \text{s.t.}\ A_{ineq}\mathbf{x} \leq \mathbf{b}_{ineq},\ A_{eq}\mathbf{x} \leq \mathbf{b}_{eq}, \tag{40}$$

is solved by using Matlab function of the following prototype

$[\mathbf{x}_{opt}, J_{opt}, \dots] = \mathit{linprog}(\mathbf{c}, A_{ineq}, \mathbf{b}_{ineq}, A_{eq}, \mathbf{b}_{\mathrm{eq}}, \mathbf{lb}, \mathbf{ub})$,

where **lb** represents lower bound vector constraint (here set to **0**), while **ub** represents upper bound vector constraint of control vector $\mathbf{x}$. The most important outputs of function are the optimal control vector $\mathbf{x}_{opt}$ (here the optimal charging power in each step for each EV along with the power of other electrical consumers) and the optimal cost function value J_{opt} (here the cost of electrical energy from the grid expressed in HRK).

4. Combined aggregate load levelling and charging cost minimization

If the grid power peaks are tend to be minimised along with the electrical energy cost (5), the optimisation problem transfers to the quadratic optimisation problem as it will be shown in this section.

4.1. Optimal control problem formulation

The problem of the grid power peak minimisation can be formulated as

$$\min \ \left\{\max \ \left\{P_{grid}(0) \quad P_{grid}(1) \quad \ldots \quad P_{grid}(N_t-1)\right\}\right\}. \tag{41}$$

Since the cumulative grid power consumption used for EV fleet charging is determined by posing demand on the target SoC values of each EV at the end of each charging period (26), and the energy demand of other electrical consumers is fixed, the following equation can be established

$$P_{grid}(0)+P_{grid}(1)+\ldots+P_{grid}(N_t-1)=E_{total}/\Delta T \ , \tag{42}$$

where E_{total} denotes the total energy taken from the grid within the time period $[0, N_t \cdot \Delta T]$.

Due to this, the problem (41) can be reduced to the following quadratic optimisation problem (see the detailed mathematical proof in Appendix).

$$\min \sum_{k=0}^{N_t-1} P_{grid}{}^2(k) \, . \tag{43}$$

4.2. Optimal control problem represented in quadratic programming (QP) form

The linear optimisation problem (7) transfers to a general quadratic optimisation problem by including a quadratic term $1/2\cdot\mathbf{x}^T Q\mathbf{x}$ to the cost function as follows [14]

$$\min \ \frac{1}{2}\mathbf{x}^T Q\mathbf{x}+\mathbf{c}^T\mathbf{x}, \quad \text{s.t.}\ A\mathbf{x}\le\mathbf{b} \, . \tag{44}$$

By considering relation (37), the cost (43) can be written as $(H\mathbf{x})^T H\mathbf{x}$, thus yielding $\mathbf{x}^T H^T H\mathbf{x}$ and $Q = H^T H$ required in (44). In this way, the minimisation of the grid peak power values is expressed as quadratic optimisation problem which can be solved by using widely available quadratic optimisation solvers.

Additionally, the optimisation problem (44) is extended with the weighting factor α in order to enable the possibility of tuning the relative significance between the quadratic cost- and linear cost-related terms.

$$\min \quad \frac{\alpha}{2}\frac{\mathbf{x}^T Q\mathbf{x}}{Q_{norm}}+(1-\alpha)\frac{\mathbf{c}^T\mathbf{x}\Delta T}{L_{norm}}, \ \text{s.t.}\ \ A_{ineq}\,\mathbf{x}\le\mathbf{b}_{ineq}\, , \ A_{eq}\,\mathbf{x}\le\mathbf{b}_{eq}, \, 0\le\alpha\le 1. \tag{45}$$

Also, the constants Q_{norm} and L_{norm} are introduced in order to normalise the quadratic- and linear cost-related terms. They are set to arbitrarily high values of the same order of magnitude as $\mathbf{x}^T Q\mathbf{x}$ and $\mathbf{c}^T\mathbf{x}\Delta T$, respectively.

This quadratic optimisation problem, with the same linear constraints (35) and (39) as in the case of the linear optimisation problem (40), is solved by using Matlab function of the following prototype

$[\mathbf{x}_{opt}, J_{opt}, \ldots] = quadprog(Q, \mathbf{c}, A_{ineq}, \mathbf{b}_{ineq}, A_{eq}, \mathbf{b}_{eq}, \mathbf{lb}, \mathbf{ub})$,

where variables have the same meaning as in the case of *linprog*(.) function used to solve linear optimisation problem (40).

5. Optimisation results

The benefits of the charging optimisation algorithm presented in the previous section are demonstrated for the case of isolated EV fleet (11 EVs, N_v = 11) and energy system ($P_{grid,limit}$ = 75 kW) described in Section 2. The EV fleet is represented by the time distributions required as inputs for the charging optimisation algorithm (see Table 2). The two-tariff electricity price model C_{el} used in this case study is shown in Fig. 2 (typically applied in Croatian energy market). The discretisation time ΔT is set to 1h, and consequently the number of discrete time steps is 24 (N_t = 24) on the considered optimisation time horizon of 24 hours. The lower and upper SoC limits of each battery are set to 0 and 1, respectively ($SoC_{\min}$ = 0, $SoC_{\max}$ = 1; see (2)). The charging (η_{ch}) and discharging efficiencies (η_{dch}) are both set to the same value of 0.95 for each EV within fleet.

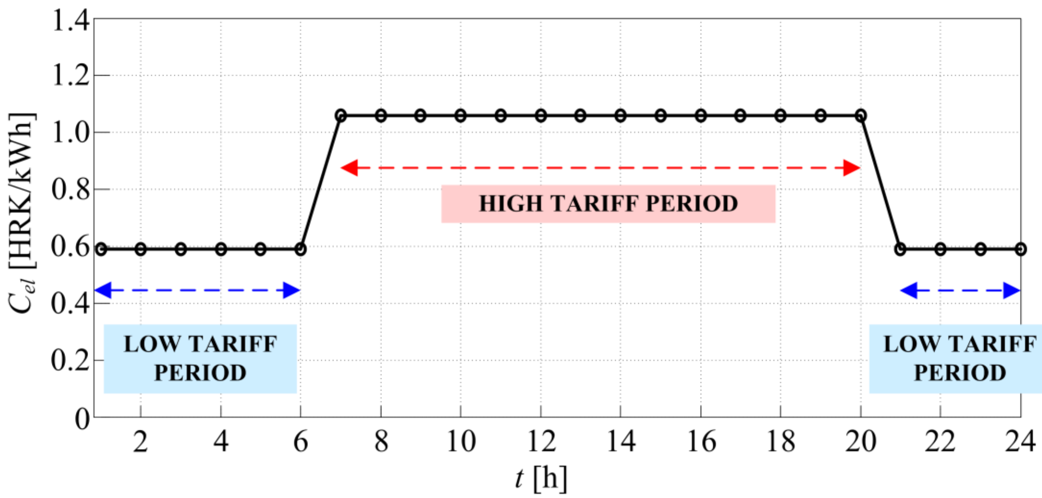

Figure 2. Two-tariff electricity price model (value given for e.g. 7h corresponds to the 6-7h time period; taken from the link http://mojracun.hep.hr/kalkulator/).

First, the LP optimisation (40) is conducted, minimising only the charging cost, while satisfying the imposed constraints. This optimisation corresponds to the QP optimisation (45), where the weighting factor α is set to 0. Table 3 shows the obtained SoC values vs. discrete time steps for each EV within the fleet. Here, the SoC value in the k^{th} column is obtained by applying the charging power, regenerative braking and demanded power values from the $(k-1)^{\text{th}}$ time step (see the state equation (1)). These SoC values ($SoC(k)$) can be interpreted as the SoC values at the end of $(k-1)^{\text{th}}$ and at the beginning of the k^{th} time step. The blue cells denote the time period when the corresponding EV is being connected to the grid and charged, while the red cells denote the periods when the EV is on the road and thus not connected to the grid. The cells denoting the periods of EVs disconnecting from the grid (dark blue cells) reveal that the requirement on the final SoC value (prior to driving) to be equal to the target one SoC_{target} (here set to 1 (100%); see (26)) is fulfilled. This requirement is omitted in the cases when an EV is not connected to the grid long enough to fully charge the battery due to the charging power limit, e.g. mini-bus B for the step k = 13, Electric train 1 for the charging period k = 16, 17. For the same reason, the final SoC values in the step k = 24 are set to the adjusted target values which are feasible (lower than 100%), and used then as initial values to calculate the SoC values in 1st time step ($SoC(0)$ = $SoC(24)$).

Table 3. Hourly time distributions of SoC values of each EV obtained by LP optimisation.

	Vehicle SoC [%] vs. discrete time steps (ΔT = 1h)																							
Vehicle	**1**	**2**	**3**	**4**	**5**	**6**	**7**	**8**	**9**	**10**	**11**	**12**	**13**	**14**	**15**	**16**	**17**	**18**	**19**	**20**	**21**	**22**	**23**	**24**
Mitsubishi iMIEV	69	73	78	84	91	**100**	69	77	86	75	87	**100**	69	73	78	84	90	**100**	69	69	86	65	83	**100**
Mitsubishi Outlander PHEV	42	37	31	29	26	21	15	10	29	46	64	81	**100**	95	89	84	79	74	68	63	58	53	50	47
VW Golf GTE	35	30	25	20	15	10	5	30	52	74	**100**	95	90	85	80	75	70	65	60	55	50	45	43	40
Mini-bus A	58	65	73	81	89	98	99	**100**	93	84	68	51	39	33	35	27	12	0	0	0	24	31	40	50
Mini-bus B	42	54	65	76	87	95	96	97	98	**100**	84	68	81	77	69	59	44	28	17	10	0	12	21	30
Nissan e-NV200	100	100	100	100	100	100	100	**100**	91	93	94	96	**100**	91	87	90	94	**100**	91	82	78	84	91	100
Electric train 1	33	45	58	70	82	94	95	97	**100**	88	76	65	53	41	29	38	47	35	24	12	0	8	15	20
Electric train 2	57	65	72	80	88	96	98	**100**	95	90	85	80	75	70	65	60	55	50	45	40	35	39	45	50
Electric ship 1	48	57	66	74	83	91	**100**	94	88	82	76	70	64	58	52	46	40	34	28	22	16	24	32	40
Electric ship 2	48	57	66	74	83	91	**100**	94	88	82	76	70	64	58	52	46	40	34	28	22	16	24	32	40
Electric ship 3	48	57	66	74	83	91	**100**	94	88	82	76	70	64	58	52	46	40	34	28	22	16	24	32	40

Table cells denoting periods when EVs are driving and thus not connected to the grid are given in red colour, while cells denoting periods when EVs are connected to the grid are given in blue colour with the dark blue ones denoting disconnecting period of the corresponding EV.

Fig. 3 shows the time distributions of the aggregate grid power which includes both the EV fleet charging power and the power of other electrical consumers for different EV fleet charging scenarios. The grid power limit is set to 75 kW (the pink line). First, uncontrolled charging (charging with maximum power until the battery is fully charged) is applied and analysed. It can be seen that in this charging approach the obtained grid power profile (the black line) violates the grid power limit during several consecutive hours, 1-4h in the morning and 23-24h in the evening. This indicates that the EV fleet charging should be controlled in order to avoid violation of the grid power limit and consequently the collapse of the corresponding energy system. Then, LP-based charging optimisation (for the case of $\alpha = 0$ in (45)), minimising only the charging cost, is conducted. The obtained power profile (the red line) now satisfies the grid power limit, and for the early morning hours it is equal to the grid power limit, thus maximally exploiting the low price of electrical energy (see electricity price in the period 1-6h in Fig. 2). Further, QP-based charging optimisation is conducted for the case of two values of α parameter. Now, by including the quadratic term from (45) into optimisation, the obtained grid power profile have significantly lower peak values. The lowest peak power value is obtained for the case of $\alpha = 1$ because in that case only the peak power-related sub-cost function is included within optimisation, i.e. the term in (45) corresponding to the charging cost is neglected, while in the case of $\alpha = 0.5$, both the peak power and the charging cost sub-cost functions are included.

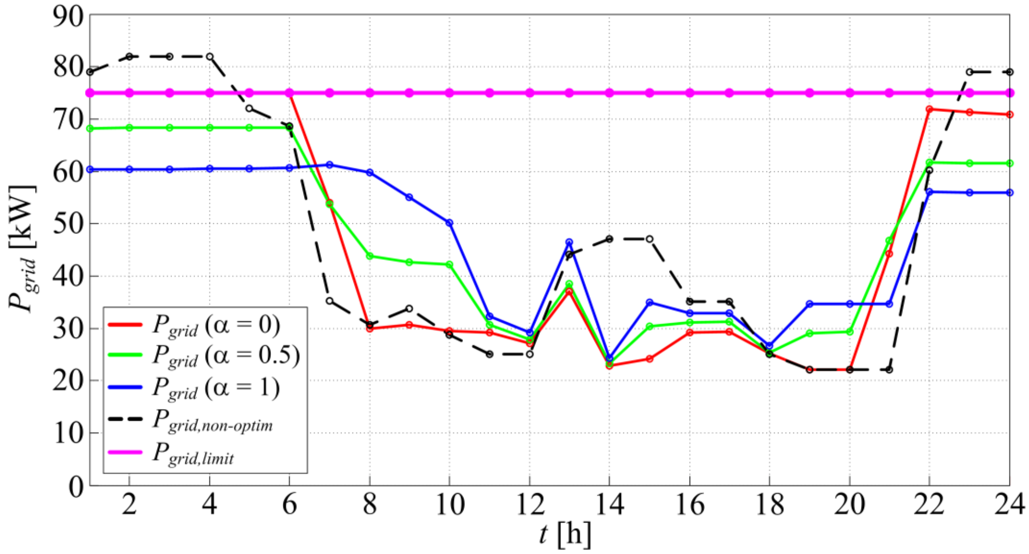

Figure 3. Aggregate grid power for different EV fleet charging scenarios.

Further, the QP optimisations (45) are conducted for different α values sampled from the interval [0, 1], for the sake of more detailed analysis of dependence of two conflicting criteria (the grid power peak $P_{grid,\max}$ and the electrical energy cost C_{total}), both aimed to be minimised, versus α parameter value. As previously shown in Fig. 3, by increasing α value, the grid power peak is decreasing, while in the same time the energy cost is increasing. Mostly uniform distribution of these criteria in Fig. 4, meaning that the relations $P_{grid,\max}$ vs. α and C_{total} vs. α are nearly linear, is obtained due to the normalisation of the linear- and quadratic-related terms in (45). In this way, the user, e.g. EV fleet owner or the isolated energy system operator, can easily tune the charging control algorithm and thus adapt it to the specific needs of the particular system.

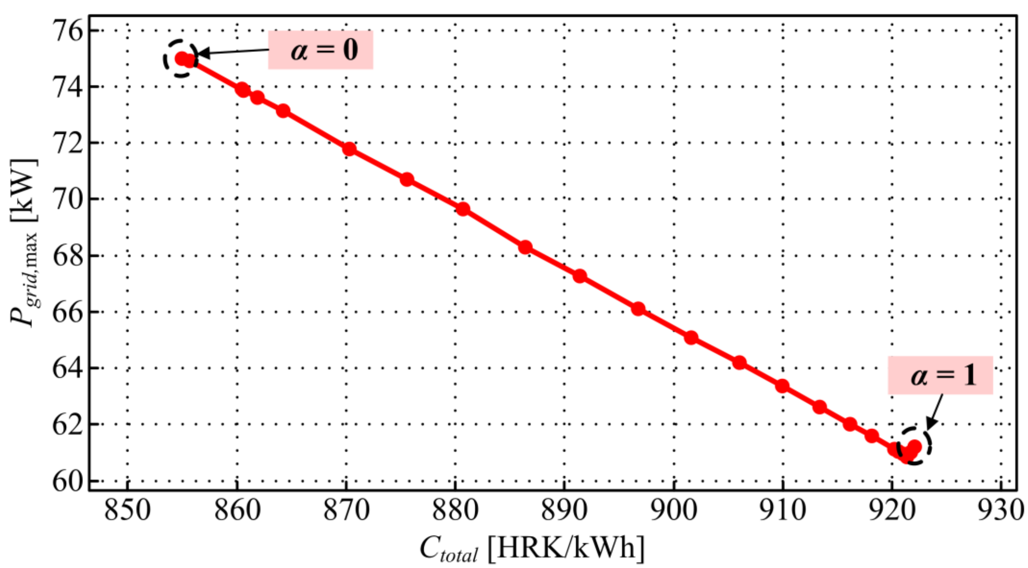

Figure 4. Two-criteria cost function (grid power peak $P_{grid,max}$ and EV fleet charging cost C_{total}) distribution for different α values.

Table 4 shows the absolute energy cost, the grid power peak and the grid power standard deviation values versus α along with the relative relations with respect to the LP optimisation results ($\alpha = 0$; percentages given in the brackets). It can be seen that by increasing the value of α from 0 to 1, the energy cost increases nearly 8%, from 855 HRK to 922 HRK, while the grid power peak and the grid power standard deviation decreases nearly 19% (from 75 kW to ≈61 kW) and 40% (from ≈22 kW to ≈14 kW), respectively. The significant reduction in the grid power peak from 75 kW to 61 kW can be also reflected in the energy cost reduction, since the grid power peak (typically three peak values are considered) is often charged by energy system operators. However, charging of the grid power peak values is not taken into account here.

Table 4. Total electrical energy cost (C_{total}), grid power peak value ($P_{grid,\max}$) and standard deviation ($P_{grid,std}$) obtained by QP optimisations for different values of parameter α.

α [-]	C_{total} [HRK]	$P_{grid,\max}$ [kW]	$P_{grid,std}$ [kW]
0.00	855.0 (0.0 %)	75.0 (0.0 %)	22.5 (0.0%)
0.10	855.7 (+0.1 %)	74.9 (-0.1 %)	22.2 (-1.2 %)
0.20	860.5 (+0.6 %)	73.9 (-1.5 %)	21.4 (-5.1 %)
0.30	864.2 (+1.1 %)	73.1 (-2.5 %)	20.7 (-8.3 %)
0.40	875.6 (+2.4 %)	70.7 (-5.8 %)	18.7 (-17.0 %)
0.50	886.4 (+3.7 %)	68.3 (-8.9 %)	16.9 (-24.8 %)
0.60	896.7 (+4.9 %)	66.1 (-11.9 %)	15.5 (-31.1 %)
0.70	906.0 (+6.0 %)	64.2 (-14.4 %)	14.5 (-35.7 %)
0.80	913.3 (+6.8 %)	62.6 (-16.5 %)	13.9 (-38.4 %)
0.90	918.1 (+7.4 %)	61.6 (-17.9 %)	13.7 (-39.2 %)
0.95	920.2 (+7.6 %)	61.1 (-18.5 %)	13.6 (-39.5 %)
0.96	920.6 (+7.7 %)	61.0 (-18.6 %)	13.6 (-39.6 %)
0.97	921.0 (+7.7 %)	60.9 (-18.7 %)	13.6 (-39.6 %)
0.98	921.4 (+7.8 %)	60.9 (-18.9 %)	13.6 (-39.6 %)
0.99	921.7 (+7.8 %)	61.0 (-18.7 %)	13.6 (-39.7 %)
1.00	922.1 (+7.9 %)	61.2 (-18.4 %)	13.6 (-39.7 %)

Percentages given in brackets denote relation between value in the corresponding cell versus LP optimisation-related value ($\alpha = 0$) in the same column.

6. Conclusion

An optimisation framework of electric vehicle (EV) fleet charging including minimisation of both the electrical energy cost and the grid power peak is proposed in this paper. Minimisation of the electrical energy cost is formulated in the linear programming (LP) optimisation form which supposes the linear cost function and the linear constraints. Then, the linear cost function is extended with the quadratic term, representing the grid power peak-related sub-cost function, thus transferring the optimal control problem from the LP to the quadratic programming (QP) one. The quadratic cost function is extended with a free parameter, which determines trade-off between typically conflicting sub-cost functions, and which can be tuned in order to meet the specific needs of the particular system, i.e. to put more emphasis on the charging cost or on the grid power peak minimisation. Effectiveness of the proposed charging algorithm is demonstrated for the case of an isolated energy system and a hypothetical EV fleet of the National park Mljet.

It is shown that the grid power limit is not violated in the case when the optimisation of EV fleet charging is conducted as opposed to the case when uncontrolled charging (charging when plugged) is applied. Furthermore, by applying the QP optimisation, the grid power peak and the grid power standard deviation decreases nearly 19% and 40%, respectively, with respect to the LP optimisation results, thus significantly contributing to the grid load levelling. However, in that case the electrical energy cost is deteriorated (increased) for nearly 8%. A good (customised) trade-off between the grid power peak and the energy cost within these ranges can be achieved by tuning the cost function weighting parameter α.

The future work is directed towards exploration of the potential of the proposed charging optimisation in terms of the grid load levelling and the energy cost reduction for a fleet with significantly higher number of EVs. In this case, the special attention will be paid to handling the infeasible constraints and the optimisation algorithm execution time (i.e. computational efficiency), which are typical problems in real-time optimisation applications.

References

1. R. Garcia-Valle and J. A. Pecas Lopes, “Electric Vehicle Integration into Modern Power Networks,” *Springer*, ISBN 978-1-4614-0134-6, 2013.

2. N. Jayasekara, P. Wolfs, and M. A. S. Masoum, “An optimal management strategy for distributed storages in distribution networks with high penetrations of PV,” *Electr. Power Syst. Res.*, vol. 116, pp. 147–157, 2014.

3. J. Tan and L. Wang, “Integration of plug-in hybrid electric vehicles into residential distribution grid based on two-layer intelligent optimization,” *IEEE Trans. Smart Grid*, vol. 5, no. 4, pp. 1774–1784, 2014.

4. S. Martinenas, A. B. Pedersen, M. Marinelli, P. B. Andersen, and C. Traeholt, “Electric vehicle smart charging using dynamic price signal,” *2014 IEEE Int. Electr. Veh. Conf. IEVC 2014*, 2015.

5. O. Sundstrom and C. Binding, “Optimization methods to plan the charging of electric vehicle fleets,” *Proc. Int. Conf. Control Commun. Power Eng.*, pp. 28–29, 2010.

6. T. K. Kristoffersen, K. Capion, and P. Meibom, “Optimal charging of electric drive vehicles in a market environment,” *Appl. Energy*, vol. 88, no. 5, pp. 1940–1948, 2011.

7. O. Sundström and C. Binding, “Flexible charging optimization for electric vehicles considering distribution grid constraints,” *IEEE Trans. Smart Grid*, vol. 3, no. 1, pp. 26–37, 2012.

8. A. Sheikhi, Sh. Bahrami, A. M. Ranjbar, and H. Oraee, “Strategic charging method for plugged in hybrid electric vehicles in smart grids; a game teoretic approach,” *Electrical Power and Energy Systems*, vol. 53, no. 1, pp. 499-506, 2013.

9. A. Di Giorgio, F. Liberati, and S. Canale, “Electric vehicles charging control in a smart grid: A model predictive control approach,” *Control Eng. Pract.*, vol. 22, pp. 147–162, 2014.

10. B. Škugor, J. Deur, “A bi-level optimisation framework for electric vehicle fleet charging management”, *Appl. Energy*, vol. 184, pp. 1332-1342, 2016.

11. B. Škugor, J. Deur, “Dynamic programming-based optimisation of charging an electric vehicle fleet system represented by an aggregate battery model”, *Energy*, vol. 92, no. 3, pp. 456-465, 2015.

12. M. Alonso, H. Amaris, J. G. Germain, and J. M. Galan, “Optimal charging scheduling of electric vehicles in smart grids by heuristic algorithms,” *Energies*, vol. 7, no. 4, pp. 2449-2475, 2014.

13. B. Škugor, J. Deur, “A Novel Model of Electric Vehicle Fleet Aggregate Battery for Energy Planning Studies”, *Energy*, vol. 92, no. 3, pp. 444-455, 2015.

14. J. Nocedal and S. J. Wright: “Numerical Optimization”, *Springer Series in Operations Research and Financial Engineering*, 2nd edition, Springer, Berlin, 2006.

Acknowledgments

It is gratefully acknowledged that this work has been done under the SOLEZ project supported by the European Union, through the Interreg CENTRAL EUROPE Programme funded under the European Regional Development Fund (more details about the project can be found on the project website www.interreg-central.eu/solez). The authors would also like to thank the staff of the National park Mljet for providing the data related to their transport and electrical energy system.

Appendix

Without loss of generality, the constraints (35) and (39) are omitted from this analysis, and the condition (42), which is equality constraint, is taken into account. The minimum of the cost function (43) is achieved in the case

$$P_{grid}(0) = P_{grid}(1) = \ldots = P_{grid}(N_t - 1), \tag{46}$$

where the perfect load levelling is obtained, i.e. no variations of the grid power.

Now, the proof for (46) follows from the Jensen’s inequality

$$\frac{f(a_1) + f(a_2) + \ldots + f(a_N)}{N} \geq f\left(\frac{a_1 + a_2 + \ldots + a_N}{N}\right), \tag{47}$$

where $f(.)$ represents a convex function. If the general input parameter a_k is replaced with $P_{grid}(k)$, and $f(.)$ is replaced with quadratic function $f(x) = x^2$, which is convex, the following relation yields by combining (42) and (47)

$$\frac{P_{grid}^{\ 2}(0) + P_{grid}^{\ 2}(1) + \ldots + P_{grid}^{\ 2}(N_t - 1)}{N_t} \geq \frac{E_{total}^{\ 2}}{\Delta T^2 \cdot N_t^{\ 2}}. \tag{48}$$

By substituting the constant grid power values from (46) with a constant denoted with r as follows $r = P_{grid}(0) = P_{grid}(1) = \ldots = P_{grid}(N_t - 1)$, the equation (42) becomes

$$N_t \cdot r = \frac{E_{total}}{\Delta T}, \tag{49}$$

while the equation (48) becomes

$$\frac{N_t r^2}{N_t} \geq \frac{E_{total}{}^2}{\Delta T^2 \cdot N_t{}^2}. \tag{50}$$

Rearrangement of (50) yields

$$N_t{}^2 r^2 \geq \frac{E_{total}{}^2}{\Delta T^2} \rightarrow N_t r \geq \frac{E_{total}}{\Delta T}, \tag{51}$$

where equality holds due to (49) and the minimum of the left-hand side of inequality (48) is achieved for the case of (46) as stated.

In summary, this proof has shown that the perfect load levelling with minimum grid power peaks is achieved by minimising the sum of quadratic terms on the left-hand side of (48). This is proved for the case when only requirement on cumulative energy demand (42) is taken into account. However, if other constraints (e.g. (35) and (39)) are also taken into account, the minimisation of the sum of quadratic functions, i.e. (43), would still lead to the minimisation of the peak power and consequently the grid load levelling.